Evolution of real contact area during stick-slip movement observed by total reflection method*

Zhijun Luo(罗治军), Baojiang Song(宋保江), Jingyu Han(韩靖宇), and Shaoze Yan(阎绍泽)†

State Key Laboratory of Tribology, Department of Mechanical Engineering, Tsinghua University, Beijing 100084, *China*

(Received 8 April 2019; revised manuscript received 11 June 2019; published online 17 September 2019)

We build an experiment system based on total reflection (TR) method to observe the evolution of real contact area of polymethyl methacrylate (PMMA) in the continual stick-slip movement. The bilateral friction is adopted to overcome the bending moment in the lateral friction movement. Besides some classical phenomena of stick-slip movement such as periodical slow increase of frictional force in sticking phase and a sudden drop when slipping, a special phenomenon that the contact area increases with the tangential force is observed, which was called junction growth by Tabor in 1959. Image processing methods are developed to observe the variation of the junction area. The results show that the center of the strongest contact region will keep sticking under the tangential force until the whole slipping, the strongest point undergoes three stages in one cycle, which are named as sticking stage, fretting stage, and cracking stage, respectively. The combined analysis reveals a physical process of stick-slip movement: the tangential force causes the increase of the real contact area, which reduces the pressure between the contact spots and finally leads to the slipping. Once slipping occurs, the real contact area drops to the original level resulting in the pressure increase to the original level, which makes the sticking happen again.

Keywords: total reflection, stick-slip, real contact area, detachment, junction growth

PACS: 46.55.+d, 42.30.Va, 78.20.Ci **DOI:** 10.1088/1674-1056/ab3f1f

1. Introduction

The stick-slip is a non-linear frictional phenomenon with alternative sticking and slipping movements, which exhibits widely in nature and daily life, such as the instability of continental plates, the squeal of brakes, and the crawling of machine tools. The stick-slip is generally harmful to the mechanical equipment because of the resulting vibration, noise, and wear.[1] Therefore, it has great practical value to research the stick-slip movements.[2,3] Early in 1930, Thomas has analyzed the interfacial intermittent motion based on the theories of static friction and Coulomb friction.[4] Subsequently, in 1939, Bowden and Leben experimentally found the alternative sticking and slipping movements between the metal interfaces at low speed, and attributed these movements to the transition between static friction and kinetic friction.[5] Since then, a great number of researchers have contributed to this field: Rabinowicz studied the stages of the stick-slip motion using a pin-on-flat tribometer and interpreted the principle of the stick-slip motion,[3,6,7] Armstrong discovered the Stribeck principle,[8,9] and Bell validated the hysteresis of friction.[10] In addition, based on experimental results, the new friction models were also proposed, such as Dahl model[11] and LuGre friction model.[12] In recent years, along with the development of observation devices, researchers found the stick-slip movement in smaller microscopic scale. For example, in atomic-scale, researchers found the stick-slip movement of a tip with nanometer order curvature on a surface, which is mainly affected by the atomic friction force.[13,14] Although some researchers proved that some traditional frictional law remains valid in smaller scale,[15] considering the factors affecting the stick-slip movement in different scale may have huge difference, thus, in this paper, we mainly focus on the traditional macroscopic scale, i.e., the stick-slip movement occurs at scale larger than microns, which is more universal in engineering.

Despite the related researches have lasted for ages, the mechanism of friction and stick-slip movement is far from a conclusion.[16] Nevertheless, there are some wildly acceptable interpretations for the friction mechanism, e.g., the friction interface is composed of many interactive asperities, which form a real contact area (the total area of the contacted asperities) that is far smaller than the nominal contact area (appearance surface area).[5] The normal force can lead to the deformation of the asperities and consequently affect the real contact area, the characteristic of interactive asperities determines the dynamic of friction.[17] Following these interpretations, in recent years, many researches deemed that directly observing the evolution of real contact area is an effective method to study the mechanism of stick-slip movement. Tuonoen studied the slip dynamics of the rubber–glass interface by an optical measurement system utilizing a high-speed camera under the glass to capture the image of real contact area. He found that the sliding motion begins from the leading edge and propagates to the trailing edge.[18] Eguchi utilized the

*Project supported by the National Natural Science Foundation of China (Grant No. 11872033) and the Beijing Natural Science Foundation, China (Grant No. 3172017).

†Corresponding author. E-mail: yansz@tsinghua.edu.cn

© 2019 Chinese Physical Society and IOP Publishing Ltd

CPB Online In-Press

white light interferometer to observe the real contact area between the rubber and glass plate, concluding that the real contact area firstly decreases with the increase of the applied tangential force and becomes approximately constant after initiation of macroscopic whole sliding.[19] In 2004, Rubinstein firstly proposed a total refection (TR) method to observe the real contact area of polymethyl methacrylate (PMMA) during the onset of friction movement, and discovered the rupture propagation.[20] Subsequently, the team of Rubinstein did a series of researches on the PMMA blocks based on the TR method,[16,21,22] they found that the onset of slip occurs through coherent detachment that propagates across the interface, and the real contact area is reduced behind a detachment front.[16] They also found that the real contact area increases logarithmically after the local rapid slip ceases before the onset of overall motion.[22] Compared with other direct observing methods, the TR method can effectively observe the real contact area between two transparent materials, and is convenient to implement. However, the previous researches using TR method mainly focused on observing the evolution of real contact area at the onset of stick-slip movement by a high-speed camera, which has great value for the seismic researches. However, the research for the evolution of real contact area variation during the continual stick-slip movement is not enough, which would be more valuable for the mechanical system.

In this paper, based on the TR method, an experiment system is constructed to observe the evolution of real contact area during continual stick-slip movement, several image-processing methods are developed to analyze the obtained images. We discover that the real contact area is determined not only by the normal force, but also by the tangential force, which is novel for the general cognition. We also research the sticking and fretting phenomenon, and discover that there are three stages before the whole slipping.

The remainder of this paper is organized as follows. Section 2 briefly introduces the principle and construction of the experiment system, Section 3 analyzes the evolution of real contact area. Section 4 traces the variation of contact area using two image-processing methods. Section 5 gives the conclusion.

2. The experimental system

According to the frictional theory, even the very smooth interface of a material is composed of a myriad of asperities with different heights.[17,20] The real contact area between two frictional materials is determined by the interconnected asperities, which is generally orders of magnitude smaller than the apparent contact area.[20] Total reflection is a classic optical phenomenon: a beam of light transmitting from the denser medium to the thinner medium will be totally reflected back into the denser medium when the incident angle is greater than the critical angle. The interface between two contact transparent materials is full of gaps except very little interconnected asperities, therefore, most of the incident beam beyond the critical angle should be totally reflected back, and the rest could transmit through the interconnected asperities. Hence, the intensity of the transmitting beam can represent the size of the real contact area, and the pattern of the transmitting beam can represent the real contact area.[20] Figure 1 is the schematic of the TR method.[23]

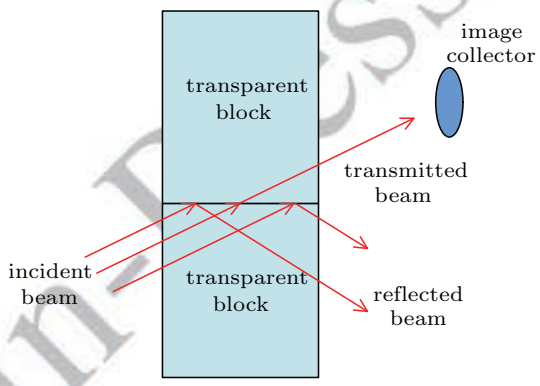


Fig. 1. The schematic of total reflect method.

In most previous researches, only two blocks are pressed together to form a single side friction as illustrated in Fig. 2, where the bending moment inevitably occurs and affects the distribution of the normal force when a tangential force is applied. As indicated in Fig. 2(b) , the supporting force increases with the length from front to rear, which may cause the detachment from front to rear. Some researchers also thought that the bending moment would be one of the major reasons causing the rupture propagation.[24] In addition, some researchers discovered that the normal force distribution would significantly affect the movement.[2] In order to eliminate the bending moment, we use three blocks, making the slipping block in the middle position, to form a bilateral friction, as shown in Fig. 3(b).

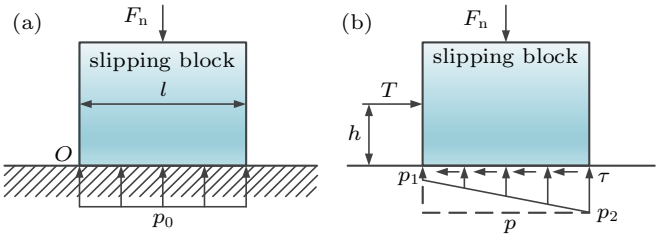


Fig. 2. The force distribution under the lateral friction: (a) the force distribution under only the normal force F_n, (b) the force distribution under the tangential force, where the supporting force p will be distributed non-uniformly to balance the torque caused by the tangential force T.

Based on the analysis above, we construct the experiment system shown in Fig. 3(a). The whole system consists of five subsystems: 1) normal force loading device comprised of an S-type force transducer, an X-type lifting platform, a stepper

motor with lead screw; 2) tangential force loading device comprised of an S-type force transducer and a high precise electric cylinder realizing micron movement; 3) bilateral friction testing components comprised of an upper fixed block, a lower fixed block, and a middle-slipping block, all blocks' material is PMMA; 4) real contact area observing module comprised of a semiconductor laser, a projection screen, and a camera; 5) data acquisition devices. Figure 3(c) is the field photo of the experimental system. The major parameters of the major devices are listed in Table 1. The sizes of the PMMA blocks are 120 mm×10 mm×30 mm, 20 mm×10 mm×20 mm, 120 mm×20 mm×15 mm for the upper block, sliding block, under block, respectively. The dimension of the middle sliding bock is smaller than that of the upper and lower blocks to ensure the pressure equilibrium. The blocks are cleaned by alcohol to weep away the contaminant before every test. The wavelength of laser light in our experiment is 650 nm. If the diameters of the contact spots are too smaller compared to the light wavelength, the transmitting light would have too large diffraction angle and severer scattering, which is hard to be captured by the camera. Thus, the observed contact area would be larger than hundreds nanometers, which means that the real contact area observed remains at macroscopic scale compared with the atomic-scale and nanoscale.

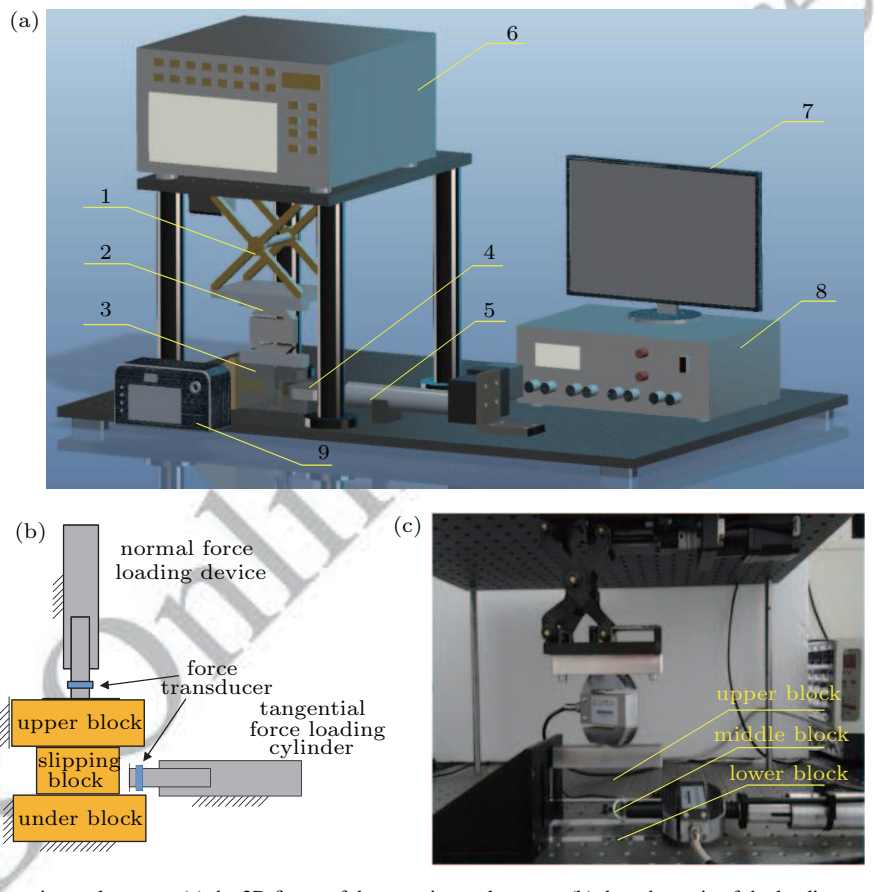


Fig. 3. Figures of the experimental system: (a) the 3D figure of the experimental system, (b) the schematic of the loading section, (c) the field photo of experiment. In panel (a), 1: X type lifting platform, 2: S type force transducer for normal force, 3: PMMA specimens consisted of three blocks, 4: S type force transducer for tangential force, 5: tangential cylinder, 6: motor driver, 7: LCD displayer, 8: data acquisition devices, 9: camera.

Table 1. Parameters of the major devices.

Device	Style	Parameters
Laser	semiconductor	650 nm
Camera	NIKON D610	24.26 million pixels
Stepper motor	400	maximum force 1 kN
Electric cylinder	600	maximum force 1 kN
Force transducer	S-type	0–500 N

3. Pre-slipping and junction growth of real contact area

In our previous study,[25,26] the relationship between normal force and real contact area is in accordance with the classical law: the real contact area is proportional to the normal force. In order to eliminate the influence of the normal force, in this section, the normal force is fixed. The major objective is to observe the evolution of the real contact area in stick-slip movement under a given normal force. Therefore, we set the normal force to 190 N, the driving velocity to 1.3 μm/s, and recorded the real contact area, frictional force, and normal force simultaneously.

To quantify the intensity of the transmitting light, we used a simple and direct method, as shown below.

The grayscale of a frame in a video can be expressed by

$$I_k(i,j) = R_k(i,j) + G_k(i,j) + B_k(i,j), \tag{1}$$

where I is the grayscale matrix of the photo, R, G, and B are the red, green, and blue grayscale matrices, respectively, i, j are the position of a pixel in the matrix, and k is the sequence number of the photo in the video.

Because the laser is red, thus the total intensity of red of the passed beam can represent the size of the real contact area. This principle can be expressed as

$$a_k = \sum_i^m \sum_j^n R_k(i,j), \tag{2}$$

where m,n are the sizes of row and column of matrix R, and a_k is the summation of grayscale of the k^{th} frame. The array $\boldsymbol{a} = (a_1, a_2, \ldots, a_k)$ can be used to depict the variation of the whole contact area.

The results of experiment are presented in Fig. 4. The example of images in one cycle are shown in Fig. 5, corresponding to the rectangle area in Fig. 4.

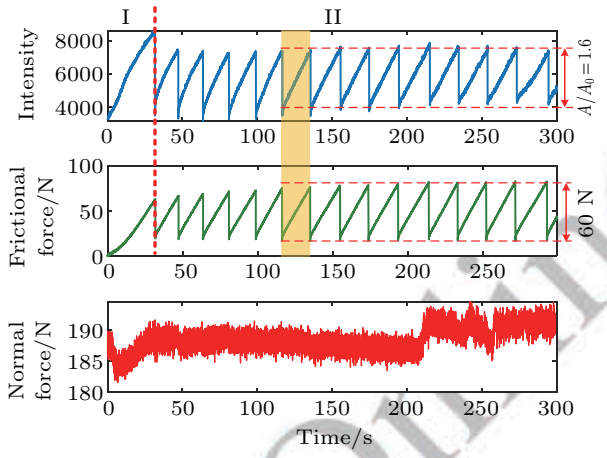


Fig. 4. The recorded data: (a) the variation of intensity corresponding to the whole contact area, which changes periodically with slow growth and sudden drop, (b) the variation of the frictional force, which is almost synchronous with the intensity, (c) the normal force, which is relatively stable around 190 N compared with the evident change of frictional force and intensity.

In Fig. 4, the real contact area and frictional force change almost simultaneously and periodically in the form of sawtooth wave during the movement, i.e., a series of a sudden drop following a slow growing, which shows a classical stick-slip movement. We can approximately divide the whole movement into 2 phases: I is the pre-slip stage, and II is the stick-slip stage. In the pre-slip stage, the frictional force and real contact area have a relative long growing time to reach the first slip. When slip occurs, the frictional force and the real contact area drop suddenly to a low level where the slip stops. After the first slip, the periodical stick-slip movement occurs, which has a shorter growing time and smaller maximum value in the real contact area. During the stick-slip movement, the ratio of the increased real contact area to the original real contact area is about 1.6, and the force increases about 60 N from 20 N to 80 N.

It is worth noticing that the real contact area grows with the increase of tangential force during the stick-slip movement. Figure 5 shows this phenomenon clearly. In the sticking phase of one cycle, the size and brightness of the red regions corresponding to the real contact area increase with the tangential force. As a traditional consensus, the real contact area increases with the normal force, which leads the increase of the frictional force, i.e., the normal force firstly determines the real contact area, and then, the frictional force. However, in our experiment, the real contact area can increase with the frictional force, but with almost no increase of normal force. The relationship in consensus does not fully hold here, i.e., without the increase of the normal force, the real contact area can also increase. In the Maegawa's research, the real contact area also increases with the tangential force during the macro stick-slip.[27] However, he did not give any interpretation.

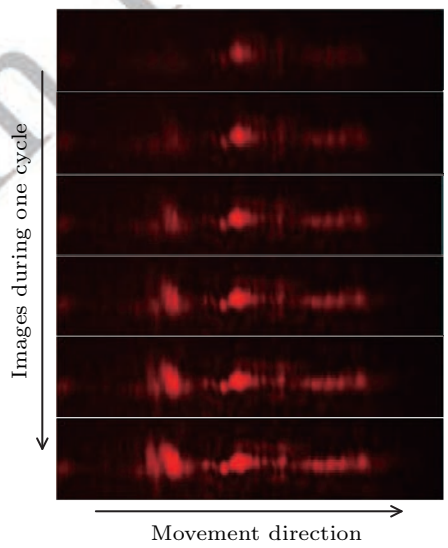


Fig. 5. Six images of sticking phase in one cycle corresponding to the rectangle area in Fig. 4: the top one is the initial image, and the bottom one is the final image in one cycle before whole slipping.

Ben-David researched the interface strengthening of a glassy physical system. He found that the real contact area of some local small part of the surface increases logarithmically after a sudden slip of the local contact area when the tangential force continually increases.[22] However, our phenomenon occurs in the whole contact area and the increase is almost linear. A more reasonable interpretation could date back to 1959, when Tabor found the junction growth in metallic friction.[28] Tabor discovered that when the tangential force increases, the real contact area increases synchronously before the slipping occurs. He concluded that this phenomenon follows the relationship[28]

$$p^2 + \alpha \cdot s^2 = p_0^2, \tag{3}$$

where p is the normal stress, s is the tangential stress in the contact region, α is an appropriate constant, and p_0 is the plastic yield pressure of the metal.

CPB Online In Press

We can rewrite Eq. (3) in the form

$$\left(\frac{F}{A}\right)^2 + \alpha \cdot \left(\frac{T}{A}\right)^2 = p_0^2, \tag{4}$$

where F is the normal force, T is the tangential force, and A is the real contact area.

If we assume that the normal force causes the initial contact area A_0, equation (4) can be converted to the form[28]

$$1 + \alpha \cdot \left(\frac{T}{F}\right)^2 = \left(\frac{A}{A_0}\right)^2. \tag{5}$$

Equation (4) explicitly illustrates that the normal force and tangential force can both cause the real contact area increase. Equation (5) indicates that under a given normal force, the increase of the tangential force can lead to an approximately linear increase of the real contact area, which gives better explanation for the linear increase in our phenomenon. When substituting the ratio of the increased contact area 1.6, the tangential force 60 N, and the normal force 190 N into Eq. (5), the coefficient α is about 15, which is in the reasonable region of 3–25 given by Tabor's experiment. Tabor measured the real contact through the conductivity of metal. However, that method is not a direct method for observing the real contact area, and cannot measure insulating substances. In 1989, Constantinou researched the junction growth of conical and spherical surfaces with several different materials, discovering that metal and plastic materials both have junction growth.[29] In 2008, Ovcharenko used an *in situ* observation rig to research the junction growth between a copper sphere and a hard sapphire flat during pre-sliding, and found that the junction growth can cause up to 45% increase in the real contact area.[30] However, these experiments are all *in situ* observation for the contact of single sphere, and only in the pre-sliding stage. In our experiment, we observed the same junction growth phenomenon at the whole contact surface during the continual stick-slipping movement, which is novel compared with previous experiments. Although, we cannot here give the deeper interpretation for the mechanism of the junction growth, our experiment remains a valuable discovery and maybe a useful method to research the relationship of junction growth and frictional movement.

4. Sticking and cracking of contact area

In Fig. 5, there are evident relative brighter areas in the image, which should correspond to the stronger contact areas. Following the theory of contact, every contact spot has a stick area and fretting area, as shown in Fig. 6,[31] which means the strongest contact point will keep stable in the sticking stage.

From Fig. 5, it is also can be observed that the position of the brightest area has no obviously changes during the movements. To verify this theory and observe the variation of junction, we designed a region growth method to trace the edge of the junction, as shown in Fig. 7. Firstly, obtain the position of the brightest point in the grayscale image. Secondly, set the brightest point as the seed point, then, carry out the region growth algorithm. Thirdly, binary the obtained region, then, contour the region to obtain the size of the brightest area. More details about the region growth method could be seen in the related book.[32]

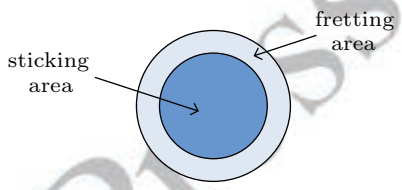


Fig. 6. The contact area of asperity under tangential force in sticking phase.

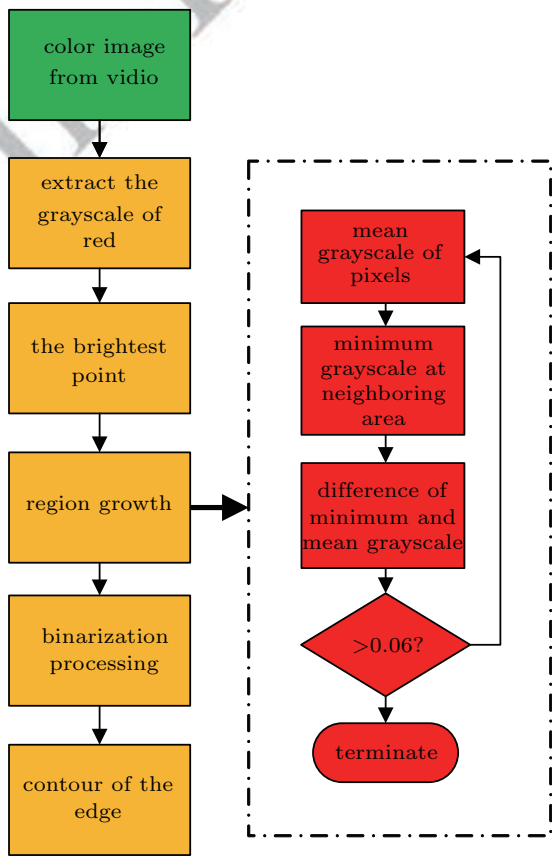


Fig. 7. The region growth method.

The results of the region growth method are shown in Fig. 8. The brightest point is located at [$x = 234$, $y = 52$]. The sequence numbers of the selected frames are 6293, 6553, 6773, which exactly contain one full pre-slip phase. The resulting images are plotted in the same coordinate with different colors, where the edges of different colors spread with an approximately common center before whole slipping. This result also confirms that the proposed region growth method is valid in observing the variation of the contact junction.

CPB Online IOP Press

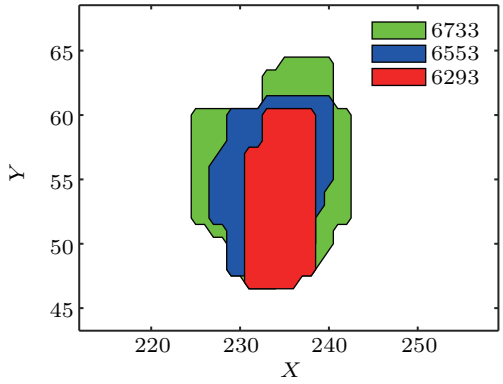


Fig. 8. The three images of brightest area in one cycle. The center of the area is in a relative stable position, having the seed point at [$x = 234$, $y = 52$].

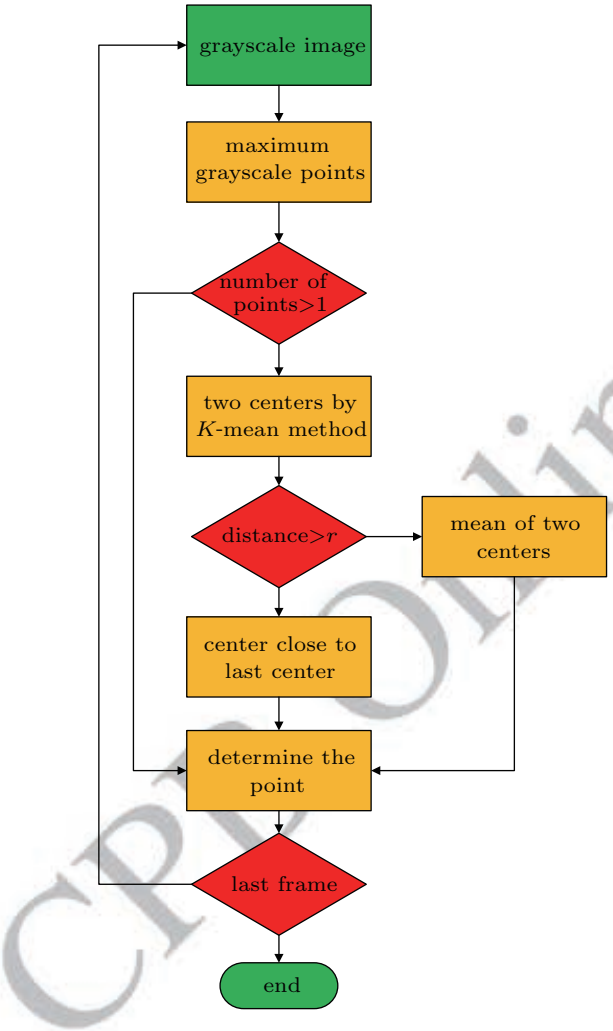


Fig. 9. The flow chart of image positioning method.

In the video, the red areas expand and move along with the movement, while the brightness is also changing, thus, it is hard to trace the movement with the traditional method such as digital image correlation (DIC)[18] because the variation of brightness and expansion of areas will disturb the result. However, it can be noted that the position of the brightest area shows no obviously changes with the movements. Theoretically, the brightest areas always correspond to the strongest intermitted asperities. Therefore, tracing the position of the brightest area would give a better detail observation for the variation of contact spot in stick-slip movement. The center point of the brightest area located by the K-mean cluster[33] method is adopted to represent the position of the strongest contact area. Because the strongest area may change during the movement, we let the number of centers equal to two. If the strongest area greatly changed, the two centers would have a large distance, if not, the centers are close, and we can deem that the two centers are in the same contact area. Based on the analysis above, we designed an image positioning method based on the K-mean cluster method as shown in Fig. 9.

Firstly, the brightest points are all picked out by grayscale value, secondly, the K-mean method is used to find the two centers of the points, If the two centers are close enough with distance less than a given critical value r, we combine the two centers, else, choose a center point close to the last center as the recorded brightest point. The results are shown in Fig. 10.

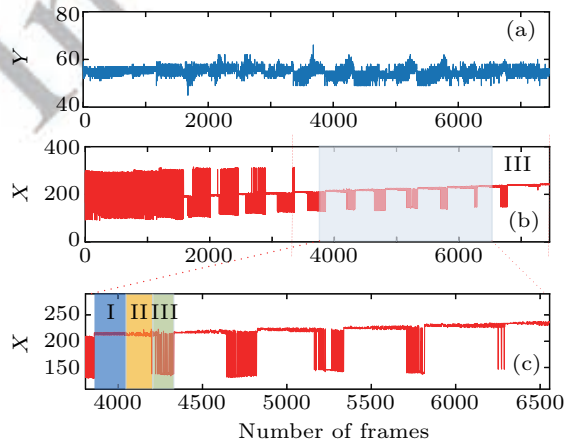


Fig. 10. The position of the brightest point in the stick-slip movement: (a) coordinate Y of the brightest point, which is in a stable position, (b) coordinate X of the brightest point, which changes periodically in the phase III of stable stick-slip movement, which can be divided into three stages in one cycle: stable sticking stage (I), where the position is relatively stable, fretting stage (II), and cracking stage (III), as shown in panel (c).

In Fig. 10(a), the position Y of the strongest contact point changes little, because it is orthogonal with the movement direction, however, in Fig. 10(b), the position X changes evidently with the movement. Before the stable phase III, the position fluctuates drastically, whereas, in phase III, the position presents a periodical variation. When zooming the phase III in Fig. 10(c), we can see that the variation can be approximately divided into 3 stages: in stage I, the strongest point is sticking, the major deformation of the contact region is elastic; with the increasing tangential force, some part of the contact regions begin fretting which causes the fluctuation of position Y of the brightest point (stage II); when the tangential force approaches the critical value, the fluctuation becomes drastically, and the rupture of the contact regions occurs, which leads to the whole slipping (stage III). These results also prove that the

CPB Online In Press

proposed image processing method is valid for the observation of contact junction in this case.

Combining the phenomenon depicted in Sections 3 and 4, we can obtain the approximate physical process of stick-slip movement. The normal force produces the original sticking area. When the tangential force increases, the real contact area increases causing the pressure acting on the contact asperities decrease. When the local pressure on some asperities decreases to a critical value, the local rupture occurs and propagates along the whole surface, which causes the sticking area unstable. When the unstable sticking area increases to some level, the whole slipping occurs, and the real contact area suddenly drops to the original level causing the pressure become high again. If the slipping velocity is lower than a critical value, high pressure will stop the slipping, the surface sticks again.

5. Conclusion

We build an experiment system based on TR method to observe the evolution of real contact area of PMMA block during the continual stick-slip movement. The bilateral friction is adopted to overcome the bending moment in lateral friction movement. In our experiment, the classical stick-slip movement is realized by a very low driving velocity under a given normal force. Besides some classical phenomena of stick-slip movement such as periodical slow increase of frictional force in sticking phase and a sudden drop when slipping, a special phenomenon that the contact area increases with the tangential force is observed, which was called junction growth by Tabor in 1959. Different with previous *in situ* observation, our research method observes the junction growth during continual stick-slip movement, which could be a useful method to research the relationship of junction growth and frictional movement.

Image processing methods are developed to observe the strongest contact area and trace the change of the strongest contact points. The results show that the strongest contact region will keep sticking under the growth of the tangential force until the whole slipping, the strongest point undergoes three stages in one cycle, which are named as sticking stage, fretting stage, and cracking stage, respectively. The meaningful results also prove that the developed image processing method is valid, and that using image-processing method to research the evolution of real contact area would be a valuable direction.

Combining the phenomenon of junction growth and the variation of strongest contact area, we propose a physical process of stick-slip movement: the tangential force causes the increase of the real contact area, which reduces the pressure between the contact spots and finally leads to the slipping. Once slipping occurs, the real contact area drops to the original level causing the pressure increase to the original level, which makes the sticking happen again.

References

[1] Ko P L and Brockley C A 1970 *Journal of Lubrication Technology* **92** 543
[2] Tian P, Tao D, Yin W, Zhang X J, Meng Y G and Tian Yu 2016 *Sci. Rep.* **6** 33730
[3] Rabinowicz E 1958 *Proc. Phys. Soc.* **71** 668
[4] Thomas S 1930 *Philos. Mag.* **9** 329
[5] Bowden F P and Tabor D 1939 *Proc. R. Soc. London* **169** 391
[6] Rabinowicz E 1951 *J. Applied Physics* **22** 1373
[7] Rabinowicz E 1995 *J. Appl. Mech.* **33** 606
[8] Armstrong-Helouvry B 1991 *Springer Science & Business Media* p. 24
[9] Armstrong-Helouvry B 1990 *Robotics and Automation 1990 IEEE International Conference* p. 1377
[10] Bell R and Burdekin M 1966 *Proc. Inst. Mech. Eng.* **181** 169
[11] Dahl P R 1976 *AIAA J.* **14** 1675
[12] Canudas C W, Olsson H and Astrom K J 1995 *IEEE Trans. Autom. Control* **40** 419
[13] Mate C M, Mcclell, G M and Erlandsson R 1987 *Phys. Rev. Lett.* **59** 1942
[14] Socoliuc A, Bennewitz R and Gnecco E 2004 *Phys. Rev. Lett.* **92** 134301
[15] Chen S H and Mi C H 2009 *Chin. Phys. Lett.* **26** 108103
[16] Rubinstein S M, Cohen G and Fineberg J 2006 *Phys. Rev. Lett.* **96** 256103
[17] Greenwood J A and Williamson J B P P 1966 *Proc. R. Soc.* **295** 1442
[18] Tuonoen A J 2014 *Tribol. Int.* **69** 70
[19] Eguchi M, Shibamiva T and Yamamoto T 2009 *Tribol. Int.* **42** 1781
[20] Rubinstein S M, Cohen G and Fineberg J 2004 *Nature* **430** 1005
[21] Rubinstein S M, Cohen G and Fineberg J 2007 *Phys. Rev. Lett.* **98** 226103
[22] David B, Rubinstein S M and Fineberg J 2010 *Nature* **463** 76
[23] Luo Z J, Song B J, Han J Y and Yan S Z 2019 *Chin. Phys. B* **28** 054601
[24] Matsuda K, Hashimoto D and Nakamura K 2016 *Tribol. Int.* **93** 523
[25] Song B J and Yan S Z 2017 *Chin. Phys. B* **26** 074601
[26] Song B J, Yan S Z and Xiangwu W K 2015 *Chin. Phys. B* **24** 014601
[27] Maegawa S, Suzuki A and Nakano K 2010 *Tribol. Lett.* **38** 313
[28] Tabor D 1959 *Proc. R. Soc. London Ser. A Math. Phys. Sci.* **251** 378
[29] Constantinou C P and Chaudhri M M 1989 *J. Mater. Sci.* **24** 4279
[30] Ovcharenko A and Halperin G and Etsion I 2008 *Wear* **264** 1043
[31] Popov V L 2010 *Contact Mechanics and Friction* (Heidelberg Berlin: Springer) p. 5
[32] Gonzaiez C, Woods E and Eddins L 2013 *Digital Image processing using Matlab* p. 301
[33] Harridan J A and Wong M A 1979 *Journal of the Royal Statistical Society* **28** 100

CPB Online First